Light-driven synthesis of hollow platinum nanospheres

Robert M. Garcia,[ab] Yujiang Song,*[a] Rachel M. Dorin,[ab] Haorong Wang,[ab] Peng Li,†[b] Yan Qiu,[ab] Frank van Swol[ab] and John A. Shelnutt*[ac]

Received (in Cambridge, UK) 30th January 2008, Accepted 3rd March 2008
First published as an Advance Article on the web 1st April 2008
DOI: 10.1039/b801695j

Hollow platinum nanospheres that are porous and have uniform shell thickness are prepared by templating platinum growth on polystyrene beads with an adsorbed porphyrin photocatalyst irradiated by visible light.

Hollow nanospheres possess tunable structural features such as shell thickness, interior cavity size, and chemical composition, leading to relatively high surface area, low density, material economy, and reduced cost compared with their solid counterparts.[1] Metallic hollow nanospheres are of special interest and importance due to various applications in biomedical,[1–3] catalytic,[4] and optical sciences.[5] Previously, nanoscale metal shells have been prepared by metal deposition onto a central core followed by core removal,[6–10] and co-assembly of metal nanoparticles with organic molecules.[11] Using unilamellar liposomes to confine the growth of metallic nanosheets within a liposomal bilayer, we recently used a tin(IV) porphyrin photocatalyst to control the sheet size to prepare spherical nanocages.[12] We now report a new method of preparing Pt nanospheres that utilizes polystyrene beads covered with a porphyrin photocatalyst to grow uniform and porous platinum nanoshells. Subsequent removal of the polystyrene core with an organic solvent results in hollow platinum nanospheres. Synthetic control over the nanoshell is realized by simply varying the concentration of platinum precursor at fixed light exposure.

Fig. 1 illustrates the synthetic scheme for the preparation of platinum hollow spheres, including evaporation induced self-assembly of hydrophobic tin(IV) octaethylporphyrin (SnOEP, Frontier Scientific) on hydrophobic polystyrene beads (Bangs Laboratories), irradiation with visible light to promote photocatalytic seeding, autocatalytic growth of seeds to form a platinum shell, and dissolution of the beads and SnOEP. The key to the synthesis is the generation of a large number of initial platinum seeds in the vicinity of the SnOEP molecules on each bead. When the seeds reach a critical size (about 2 nm), they become catalytic and autocatalyze the further reduction of platinum complex and growth of the seeds into dendrites until the Pt complex is completely consumed.[13,14] Consequently, many neighbouring small dendrites join to evenly cover the beads and form the spherical platinum nanoshells.

In a typical synthesis, 1 mL aqueous suspension of beads with an average diameter of 99 nm (10.2 wt% solid content) is mixed with 9 mL of ethanol containing 17.6 mg SnOEP in a round-bottom flask. Subsequently, ethanol and water in the mixture are removed by rotary evaporation resulting in pink flakes that peel off the glass wall. The flakes of polystyrene beads with adsorbed SnOEP are collected and further dried overnight in a desiccator under vacuum. Because SnOEP molecules are hydrophobic, they are expected to adsorb onto the hydrophobic surface of the beads. 1.76 mL of 20 mM aged K_2PtCl_4 aqueous solution and 0.24 mL water from a Barnstead Nanopure system (Chesterland, OH) are mixed with 2 mg of the dried beads coated with SnOEP. The mixture is sonicated for an hour in a water-bath cleaner to well suspend the beads. Next, 2 mL of 150 mM ascorbic acid (AA) aqueous solution is added to the above mixture. A representative UV–visible spectrum (Fig. 2, spectrum a) of the initial reaction system ($[K_2PtCl_4]$ = 8.8 mM, [AA] = 75 mM, $\sim 6.2 \times 10^{12}$ beads mL^{-1}, [SnOEP] = $\sim$10.4 μM) shows a characteristic absorption peak at 402 nm for SnOEP molecules. The high sloping baseline reflects light scattering caused by the presence of the colloidal beads. The weaker absorption features of the Pt complex in spectrum a can be identified with the aid of the spectrum b (Fig. 2) of the pure aqueous Pt complex (8.8 mM).

The reaction system reacts under stirring and irradiation by two incandescent light sources (800 nmol cm^{-2} s^{-1}) for 30 minutes. After discontinuation of the stirring, a colourless transparent supernatant with a black precipitate at the bottom is observed, suggesting that the reduction reaction has gone to completion and the beads have settled out. The UV–visible

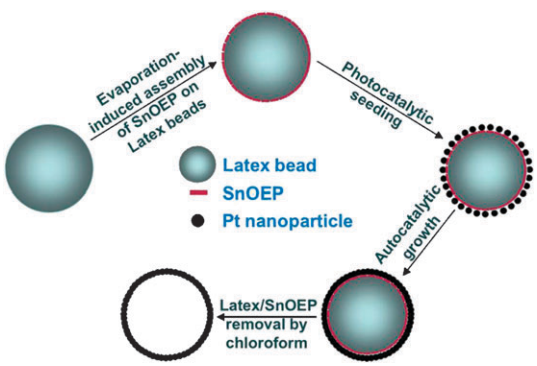

Fig. 1 Diagram of steps for the synthesis of hollow platinum nanospheres.

[a] *Advanced Materials Laboratory, Sandia National Laboratories, Albuquerque, NM 87106. E-mail: ysong@sandia.gov; Fax: +1 505 272-7077; Tel: +1 505 272-7078*
[b] *Departments of Chemistry, Chemical & Nuclear Engineering, and Earth & Planetary Sciences, University of New Mexico, Albuquerque, NM 87131*
[c] *Department of Chemistry, University of Georgia, Athens, GA 30602. E-mail: jasheln@unm.edu; Fax: +1 505 272-7077; Tel: +1 505 272-7160*
† Currently at Advanced Technology Development, Intel Corp., Chandler, AZ.

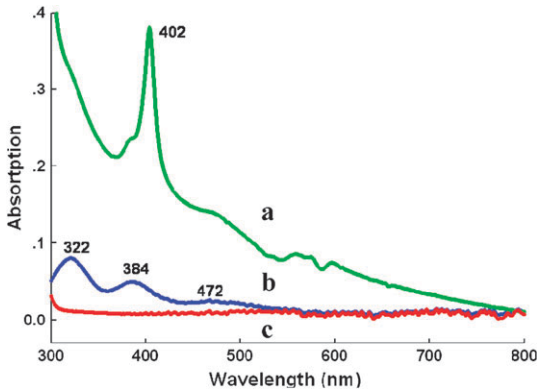

Fig. 2 UV–vis spectrum of a typical reaction system before (green) and after reaction (red). To identify the absorption maxima of the platinum complexes, a characteristic UV–vis spectrum of aqueous platinum salt is included (blue).

spectrum of the supernatant obtained is shown in spectrum c of Fig. 2; it shows that the absorption peaks (and the light scattering) disappear after the reaction and confirms that the reduction reaction is complete. The SnOEP-modified beads precipitate out likely as a result of the heavy platinum coating.

Transmission electron microscopy (TEM) of the black precipitate reveals that platinum shells with polystyrene cores are obtained as shown in Fig. 3a. The platinum core-shell nanostructures have a uniform shell thickness of 12.4 ± 1.8 nm based on the measurement of 100 individual shells in different areas (Fig. 3b). The monodispersity of the nanoshell thickness

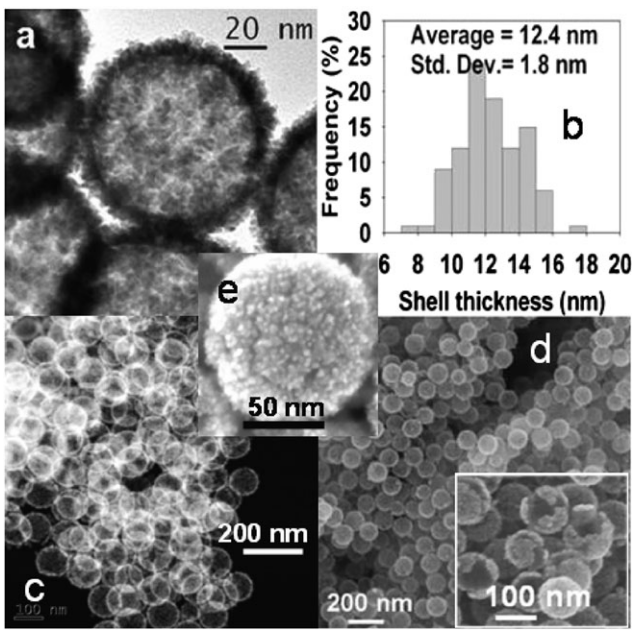

Fig. 3 (a) Bright-field TEM image of platinum nanoshells coated on polystyrene beads; (b) Plot of frequency *versus* thickness for 100 randomly selected sections of platinum nanoshells with average size and standard deviation given in the plot; (c) HAADF scanning TEM image of hollow platinum nanospheres after chloroform treatment; (d) and (e) SEM images of hollow platinum nanospheres at different magnifications after chloroform etching. (Inset: SEM image of several partially broken spheres with hollow interior).

arises from the photocatalytic seeding process, which rapidly generates a large number of initial seeds on each bead according to the simplified reactions:

$$\mathrm{SnOEP} + h\nu \rightarrow \mathrm{SnOEP}^*$$

$$\mathrm{SnOEP}^* + \mathrm{ED} \rightarrow [\mathrm{SnOEP}]^{-\bullet} + \mathrm{ED}_{ox}$$

$$2[\mathrm{SnOEP}]^{-\bullet} + \mathrm{Pt}^{2+} \rightarrow 2\mathrm{SnOEP} + \mathrm{Pt}^0$$

where AA is used as the electron donor (ED) and Pt^{2+} is provided by aged aqueous platinum salt (K_2PtCl_4).

The platinum seeds are primarily produced in the first 2–3 minutes of irradiation by photocatalysis. During this initial period of seed formation, the contribution of the direct chemical reduction of the Pt complex by AA is negligible.[13,15] Afterwards, the reaction mixture turns black, shutting down the photocatalytic seeding process since there is not enough light available to drive significant photocatalytic reduction. The seeds produced in the initial period then grow autocatalytically for almost the same length of time and thus achieve similar final sizes. The nanoshells are formed by the joining of these complex-shaped particles, which appear to be dendrites[13,15] (Fig. 3a and e); consequently, the shells are porous due to incomplete platinum coverage of dendrites on the beads.

The central polystyrene core and adsorbed SnOEP can be readily dissolved away by placing the dried samples into chloroform for at least 5 minutes under ambient conditions. Most of the platinum nanoshells are intact after chloroform treatment as shown in Fig. 3c, suggesting that the platinum shells are well formed even for this porous structure. Even more convincingly, the TEM images in Fig. 3a and c shows that the thickness of the platinum shells is uniform from shell to shell owing partly to the enhanced contrast of high-angle annular dark-field (HAADF) scanning TEM.[16] A scanning electron microscopy (SEM) image (Fig. 3d) confirms the structural integrity of platinum nanoshells after central core removal. The inset of the SEM image shows an atypical region with several broken platinum nanospheres, demonstrating that the shell interiors are hollow and that central core removal by chloroform is effective. The presence of nanopores in the platinum shells likely facilitates the removal of the chloroform-dissolved polystyrene and SnOEP.

To demonstrate the importance of the photocatalytic seeding for successful preparation of hollow platinum nanospheres, a control experiment was performed in the absence of SnOEP, while holding all the other reaction parameters constant ($[K_2PtCl_4] = 8.8$ mM, $[AA] = 75$ mM, $\sim 6.2 \times 10^{12}$ beads mL^{-1}). Unlike the SnOEP-decorated beads, the reaction system begins to turn black after 25 minutes of irradiation. TEM analysis (Fig. 4) reveals that all the platinum metal has grown onto polystyrene beads, but the platinum nanostructures range widely in size from 3 to 50 nm in diameter. The reason for the poor coverage of the beads is that in the absence of SnOEP and/or light only chemical reduction of the Pt complex by AA occurs. This only provides a relatively small number of seeds, producing relatively large Pt dendrites. Moreover, the dark seeding process is slow and continuous,[13] giving a broad distribution of dendrite sizes. That is, compared with photocatalytically formed seeds that are produced in a short initial time

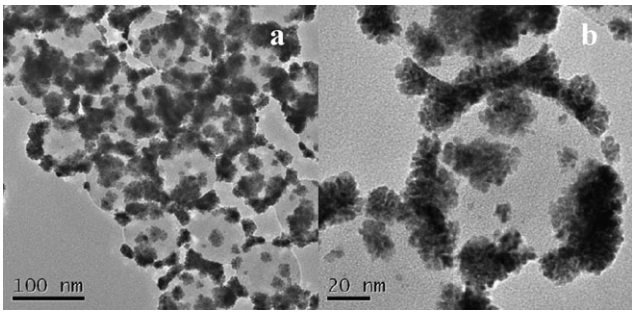

Fig. 4 TEM images of Pt nanostructures grown on polystyrene beads without SnOEP at low (a) and high (b) magnifications.

interval, seeds produced chemically at different times have varied growth periods leading to a final broad size distribution. In addition, because of the small number of seeds produced chemically, the dendrites, although larger (up to 50 nm), do not adequately bridge to adjacent dendrites to form complete shells. A similar result is obtained in an experiment using SnOEP decorated beads but without light irradiation, giving TEM images (not shown) like those shown in Fig. 4. These experiments demonstrate that the SnOEP-based photocatalytic seeding is crucial for the preparation of high-quality hollow platinum nanospheres. Additionally, it appears that platinum metal prefers nucleating and growing on the hydrophobic surface of polystyrene beads. This phenomenon agrees well with our previous observations using liposomes to template platinum growth, for which platinum metal preferably nucleates and grows within the hydrophobic liposomal bilayer.[12,17]

An important factor that influences the quality of the generated hollow platinum spheres is the amount of SnOEP photocatalyst coverage on the beads. In our typical synthesis, the optimum surface area of the SnOEP molecules is calculated to be approximately 10 times that of the beads. This calculation compares the geometrical area of the spheres with an average diameter of 99 nm to the area of the SnOEP molecules, which are approximately 2 nm × 2 nm assuming the square planar molecule lies flat on the bead. Less SnOEP results in incomplete platinum coatings on the surface of the beads, while excess SnOEP leads to the formation of platinum not deposited on surface of the beads. The latter may occur because some SnOEP molecules are not adsorbed and function as isolated competing nucleation sites.

Relying on the above understanding of the photocatalytic reaction, the thickness of the shells should be controllable by varying the amount of platinum complex available for growth and the light exposure. Indeed, the coverage of platinum on polystyrene beads can be controlled by simply reducing the concentration of aqueous salt from 8.8 to 4.4, 2.2, 0.55, and 0.28 mM at constant light exposure. As shown in Fig. 5, with the decrease of Pt(II) concentration the coverage on the polystyrene beads becomes increasingly incomplete as the size of the dendrites are reduced. At the lowest Pt concentrations, the fewer connections evident in the images would preclude shell formation. In particular, for 4.4 mM Pt salt, more than 50% of the hollow platinum nanospheres fall apart after dissolution of the beads. In contrast, 8.8 mM Pt salt produces intact shells with few broken ones (Fig. 3c and d). This demonstrates that delicate control over shell thickness is practicable and that some control over the porosity of the Pt nanoshells is possible. At the lowest

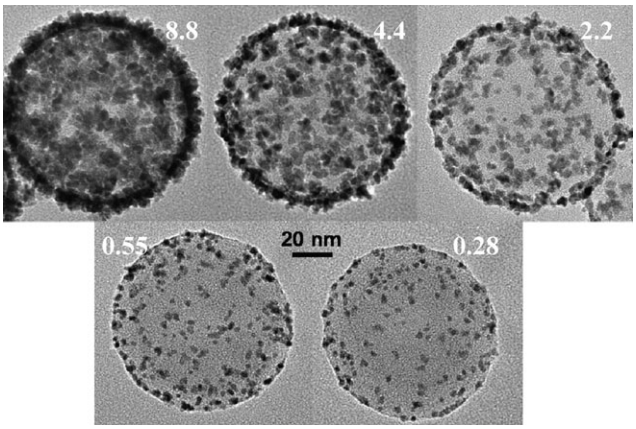

Fig. 5 Bright-field TEM images of platinum nanostructures grown on polystyrene beads in the presence of 8.8, 4.4, 2.2, 0.55, and 0.28 mM platinum complex, respectively.

concentrations of 0.55 and 0.28 mM Pt salt, abundant Pt nanoparticles are observed on the beads. However, to attain intact Pt nanoshells thinner than 12 nm, many small dendrites would be required to allow them to join with neighbouring ones to form the shell. These thin shells might be obtained by using a stronger light source to increase the seed density on the beads.

This work was partially supported by the Office of Basic Energy of Sciences, US Department of Energy. Sandia is a multiprogram laboratory operated by Sandia Corporation, a Lockheed Martin Company, for the United States Department of Energy's National Nuclear Security Administration under Contract DEAC04-94AL85000.

Notes and references

1 Y. D. Yin, R. M. Rioux, C. K. Erdonmez, S. Hughes, G. A. Somorjai and A. P. Alivisatos, *Science*, 2004, **304**, 711.
2 L. R. Hirsch, R. J. Stafford, J. A. Bankson, S. R. Sershen, B. Rivera, R. E. Price, J. D. Hazle, N. J. Halas and J. L. West, *Proc. Natl. Acad. Sci. U. S. A.*, 2003, **100**, 13549.
3 L. R. Hirsch, J. B. Jackson, A. Lee, N. J. Halas and J. West, *Anal. Chem.*, 2003, **75**, 2377.
4 S. W. Kim, M. Kim, W. Y. Lee and T. Hyeon, *J. Am. Chem. Soc.*, 2002, **124**, 7642.
5 Y. J. Xiong, B. Wiley, J. Y. Chen, Z. Y. Li, Y. D. Yin and Y. N. Xia, *Angew. Chem., Int. Ed.*, 2005, **44**, 7913.
6 P. Jiang, J. F. Bertone and V. L. Colvin, *Science*, 2001, **291**, 453.
7 H. P. Liang, H. M. Zhang, J. S. Hu, Y. G. Guo, L. J. Wan and C. L. Bai, *Angew. Chem., Int. Ed.*, 2004, **43**, 1540.
8 E. Prodan, C. Radloff, N. J. Halas and P. Nordlander, *Science*, 2003, **302**, 419.
9 Y. G. Sun and Y. N. Xia, *Science*, 2002, **298**, 2176.
10 Y. Vasquez, A. K. Sra and R. E. Schaak, *J. Am. Chem. Soc.*, 2005, **127**, 12504.
11 M. S. Wong, J. N. Cha, K. S. Choi, T. J. Deming and G. D. Stucky, *Nano Lett.*, 2002, **2**, 583.
12 Y. J. Song, R. M. Garcia, R. M. Dorin, H. R. Wang, Y. Qiu and J. A. Shelnutt, *Angew. Chem., Int. Ed.*, 2006, **45**, 8126.
13 Y. J. Song, Y. Yang, C. J. Medforth, E. Pereira, A. K. Singh, H. F. Xu, Y. B. Jiang, C. J. Brinker, F. van Swol and J. A. Shelnutt, *J. Am. Chem. Soc.*, 2004, **126**, 635.
14 E. Greenbaum, *J. Phys. Chem.*, 1988, **92**, 4571.
15 Y. J. Song, Y. B. Jiang, H. R. Wang, D. A. Pena, Y. Qiu, J. E. Miller and J. A. Shelnutt, *Nanotechnology*, 2006, **17**, 1300.
16 Z. L. Wang, *Adv. Mater.*, 2003, **13**, 1497.
17 Y. J. Song, W. A. Steen, D. Pena, Y. B. Jiang, C. J. Medforth, Q. S. Huo, J. L. Pincus, Y. Qiu, D. Y. Sasaki, J. E. Miller and J. A. Shelnutt, *Chem. Mater.*, 2006, **18**, 2335.